M06e - Gyroscope with three axes

Lab Group 6: [redacted] *(50%)*, Jordan Grey([redacted]) *(50%)*

November 12, 2024

Abstract

This study investigates the rotational dynamics of a gyroscope, examining the system's exposure to different external factors. The first experiment with an additional mass reveals the moment of inertia of the gyro disk, using multiple computational methods. Their corresponding values to are $I_3^{\alpha} = (0.01021 \pm 1.754 \cdot 10^{-4})Kgm^2$, for angular acceleration α and $I_3^{\omega} = (0.01236 \pm 3.768 \cdot 10^{-4})Kgm^2$, for angular velocity ω. They both deviates from the theoretical value of $I_3^T = (0.01172 \pm 1.877 \cdot 10^{-5})Kgm^2$. The friction coefficients averaged across trials was $b = (0.006223 \pm 4.5 \cdot 10^{-5})s^-1$. The torque-derived moments of inertia were $I_3^1 = (0.03043 \pm 0.002033)Kgm^2$ and $I_3^2 = (0.03263 \pm 0.005411)Kgm^2$. It is observed a weak linearity between rotation and nutation frequencies, obtaining ξ of 0.1607 ± 0.03165 weakly correlated with measured data, $r^2 = 0.617$. Also, it was obtained $I_1 \approx (0.0087 - 0.0106)Kg \cdot m^2$ from I_3, having a distant value from $I_1^{\omega} = (0.01065 \pm 4.355 \cdot 10^{-4})Kgm^2$, $I_1^T = (0.0101 \pm 2.758 \cdot 10^{-4})Kgm^2$ and $I_1^{\alpha} = (0.008797 \pm 2.835 \cdot 10^{-4})Kgm^2$.

1 Introduction

This report analyses the characteristics of a gyroscope, focusing on understanding its behavior in the gravitational field. By analyzing factors such as precession, angular velocity and effects of external torques, the goal is to understand the physics of gyroscopic motion. The impact different conditions have to precession, rotation and nutation and to investigate the relationship between the moment of inertia of the gyroscope and its resistance to external forces. This report aim to determine quantitative relationships between the torque, angular momentum and precession frequency to provide further insight into the dynamics of gyroscopic phenomenon, such as stabilization and three-axis oscillations, beyond a theoretical basis. The report is separated by four tasks, exposing the gyroscope to different initial conditions and experimental setups, in order to offer a complex scientific understanding.

2 Theoretical Basis

2.1 General Information

A gyroscope is a device that utilizes the principle of angular momentum to maintain its orientation relative to the Earth's axis or resist changes in its orientation. The angular momentum is given by:

$$\vec{L} = I_{123}\vec{\omega} \tag{1}$$

Where:

$$I_{123} = \text{Moment of Inertia Tensor}(Kg \cdot m^2)$$

$$\vec{\omega} = \text{Angular Velocity of the Object}(s^{-1})$$

For the same object, the moment of inertia will vary depending on the axis of rotation. In general, moments of inertia are not identical unless the object is symmetric about the axes in question. The moment of inertia tensor provides a compact representation of all the moments of inertia of an object, encapsulating the resistance to rotational motion about different axes. The products of inertia represents how the mass distribution affects rotation across the different axes [3].

$$I_{123} = \begin{bmatrix} I_{11} & I_{12} & I_{13} \\ I_{21} & I_{22} & I_{23} \\ I_{31} & I_{32} & I_{33} \end{bmatrix} \tag{2}$$

Where:

$$I_{11}, I_{22}, I_{33} = \text{Moment of Inertia about 1st-axis, 2nd-axis and 3rd-axis respectively } (Kg \cdot m^2)$$

$$I_{12}, I_{13}, I_{21}, I_{23}, I_{31}, I_{32} = \text{Products of Inertia}(Kg \cdot m^2)$$

Considering the rotational symmetry of the rigid body, the coordinate system of the principal axes of the rigid body, the moment of inertia tensor takes a diagonal form:

$$I'_{123} = \begin{bmatrix} I_{11} & 0 & 0 \\ 0 & I_{22} & 0 \\ 0 & 0 & I_{33} \end{bmatrix} \tag{3}$$

If the gyroscope is rotating around the 3rd-axis, the moment of inertia I_{33} is the rotational inertia about that 3rd-axis. This value depends on the mass distribution of the gyroscope, with $I_{22} = I_{11}$ as the gyroscope has axial symmetry. For a solid disk, it is typically calculated as [1]:

$$I_{33} = \frac{1}{2} M R^2 \tag{4}$$

Where:

$$M = \text{Mass of the Disk}(kg)$$

$$R = \text{Radius of the Disk}(m)$$

The other elements of the inertia tensor (such as I_{12}, I_{13}) are zero, because the gyroscope is symmetric about the 3rd-axis and the coordinate axes are aligned with the principal axes of the gyroscope. Therefore, there are no mixed moments of inertia between different axes in this case.
The fundamental equation of rotational motion is the link between the angular momentum and torques, it is given by:

$$\vec{\tau} = \frac{d\vec{L}}{dt} \tag{5}$$

Where:

$$\vec{\tau} = \text{Torque acting on Gyro}(N \cdot m)$$

$$t = \text{Time}(s)$$

Now, a second coordinate system is introduced, namely the principal axes system, which is rigidly fixed to the body of the gyroscope. This system rotates with respect to the laboratory system and has an instantaneous angular velocity $\vec{\omega}$ and an angular momentum vector $\vec{L_P}$. By analyzing the relationship between rotating reference frames, one can show that the angular momentum vectors in the two reference frames are related by [1]:

$$\frac{d\vec{L}}{dt} = \frac{d\vec{L_P}}{dt} + \vec{\omega} \times \vec{L_P} \tag{6}$$

However, this can be used with use of Eq. 1, to define L_P in a different form:

$$\vec{L_P} = I'_{123}\vec{\omega} \implies \begin{bmatrix} L_1 \\ L_2 \\ L_3 \end{bmatrix} = {I_{123}}' \begin{bmatrix} \omega_1 \\ \omega_2 \\ \omega_3 \end{bmatrix} \implies \begin{bmatrix} L_1 \\ L_2 \\ L_3 \end{bmatrix} = \begin{bmatrix} I_1\omega_1 \\ I_2\omega_2 \\ I_3\omega_3 \end{bmatrix} \tag{7}$$

$$\vec{\omega} \times \vec{L_P} = \begin{bmatrix} (I_3 - I_2)\omega_2\omega_3 \\ (I_1 - I_3)\omega_1\omega_3 \\ (I_2 - I_1)\omega_1\omega_2 \end{bmatrix} \tag{8}$$

The torques are expressed using Euler's equations [3]:

$$\tau_1 = I_1 \frac{d\omega_1}{dt} + (I_3 - I_2)\omega_2\omega_3 \tag{9}$$

$$\tau_2 = I_2 \frac{d\omega_2}{dt} + (I_1 - I_3)\omega_3\omega_1 \tag{10}$$

$$\tau_3 = I_3 \frac{d\omega_3}{dt} + (I_2 - I_1)\omega_1\omega_2 \tag{11}$$

The terms $(I_i - I_j)\omega_i\omega_j$ are gyroscopic coupling terms that arise due to the non-zero angular velocities in multiple directions. They indicate how rotation around one axis can influence the rate of change of angular momentum around another axis due to differences in moments of inertia. If there is no external torque, $\vec{\tau} = \vec{0}$, the object will exhibit precession or nutation depending on the initial angular velocity and the moments of inertia.

2.2 Acceleration of the disk by a falling mass

Consider the disk with the moment inertia from Eq. 4 ($I_3 \implies I_z$), rotating about a fixed axis through its center of mass, perpendicular to the large face of the disk. A massless bobbin with radius r is fixed to the disk. A massless thread is wound around the bobbin, and a weight is attached to the end of the thread.
The weight falls under the influence of gravity, starting from rest and causes rotation of the disk. The force transmitted to the disk in the thread is tension. The relationship between the linear acceleration of the weight, the angular acceleration of the disk and the tension force is given by [1]:

$$\tau = I_z\alpha = rT, \text{ with } a = r\alpha \tag{12}$$

$$m\alpha = mg - T \tag{13}$$

From Newton's equations α can be found with use of Eq. 12 to be:

$$h = v_o t + \frac{1}{2}at^2, v_0 = 0 \implies a = \frac{2h}{t^2} \implies \alpha = \frac{2h}{rt^2} \tag{14}$$

Rearranging Eq. 13 and substituting in Eq. 14 I_3 is determined to be:

$$I_3 = m_z r^2 (\frac{gt^2}{2h} - 1) \tag{15}$$

The moment of inertia can also be determined from the rotational speed, with use of the conservation of energy [3]:

$$mgh = \frac{1}{2}(I_z\omega^2 + mv^2) = \frac{1}{2}(I_z\omega^2 + mr^2\omega^2) \implies I_z = \frac{2mgh}{\omega^2 - mr^2} \tag{16}$$

Where:

$m =$ Mass of the Weight(Kg)
$r =$ Radius of the Bobbin(m)
$T =$ Tension in the Thread(N)
$\alpha =$ Angular Acceleration(s^{-2})
$a =$ Linear Acceleration(m/s^2)
$I_z =$ Moment of Inertia about z-axis$(Kg \cdot m^2)$
$g =$ Gravitational Acceleration(m/s^2)
$h =$ Fall Height(m)
$v =$ Velocity of the Weight(m/s)

2.3 Damping

To quantify the influence of friction, it is first assumed the damping of the angular velocity about the arm of the gyroscope ω_3 will be exponential. With this assumption a damped rotational model [1]:

$$\frac{d\omega}{dt} = -b\omega(t) \tag{17}$$

$$\omega(t) = \omega_0 e^{-bt} \tag{18}$$

can be used to determine the damping constant b. The value of the damping constant is attributed to frictional forces of the system. For the case of a gyroscope that rotates only about the arm of the gyroscope, the frictional forces of the system is a result of a frictional torques produced by the normal force acting on the interfaces between: the disk and the ball bearing, the ball bearing and the bearings inside, and the ball-bearing and the rod. For simplicity these frictional torques will be absorbed into a single frictional torque that acts on the surface between the disk and ball bearing, with radius $r_s = (16 \pm 1)mm$. This frictional torque opposes the angular momentum of the system with a resulting equation:

$$-I_3\alpha = \tau_f = \mu N r_s \iff \alpha = -b\omega(t)$$

$$\implies \mu(w) = \frac{I_3 b\omega(t)}{N r_s} \tag{19}$$

Where:

$$r_s = \text{Radius of surface between disk and bearing}(m)$$
$$N = \text{Normal Force on bearing}(N) = gM_{disk}$$

Note that in Eq. 19 the friction coefficient is dependent on the $\omega(t)$ and changes as $\omega(t)$ varies over time, i.e. $\mu(w,t)$. This is a direct result of assuming the deceleration due to friction is exponential in nature.

2.4 Precession

Consider a symmetric gyroscope consisting of a gyro disk, an axis, and counterweights, all supported at the center of mass. When the gyro disk rotates about its figure axis, the angular velocity and angular momentum are parallel. Since no external torque is acting on the system, the angular momentum remains conserved, and the figure axis of the gyroscope stays aligned with the direction of the angular momentum. In this case, the angular momentum vector points horizontally.
Now, suppose a small mass m is fixed to the axis at a distance z from the center of mass. This configuration generates a torque, perpendicular to the angular momentum, given by the cross product [2]:

$$\vec{\tau} = \vec{r} \times \vec{G}, \text{ with } \vec{G} = m\vec{g} \tag{20}$$

Where:

$$\vec{r} = \text{Vector of the z distance}(m)$$

$$\vec{G} = \text{Weight of Additional Mass}(N)$$

The torque causes a change in the direction of the angular momentum, but it does not affect its magnitude. As a result, the angular momentum vector precesses around the vertical axis with angular velocity. During a small time interval, the angular momentum changes direction by an angle $d\phi$, such that the angular frequency of the precession is given by [3]:

$$d\phi = \frac{dL}{L} \tag{21}$$

$$\Omega_P = \frac{d\phi}{dt} = \frac{1}{L}\frac{dL}{dt} = \frac{\tau}{L} \tag{22}$$

Where:

$$\Omega_P = \text{Angular Frequency of the Precession}(s^{-1})$$

$$L = \text{Magnitude of the Angular Momentum}(m^2 kg/s)$$

The motion of the angular momentum vector in response to an external torque is called precession. It occurs with angular velocity and is driven by a torque. In the case of a horizontally adjusted gyroscope, an additional mass fixed at a distance from the vertical rotation axis, generates a torque given by:

$$\tau = mgz \tag{23}$$

The angular momentum of the gyroscope is given by:

$$|\vec{L}| = |I\vec{\omega}| \implies L = \sqrt{{I_1\Omega_P}^2 + {I_3\Omega_3}^2} \tag{24}$$

Where:

$$\omega_3 = \text{Angular Velocity along the Figure Axis}(s^{-1})$$

Since $\Omega_P << \omega_3$ the first term on the right hand side of Eq. 24 is neglected.

2.5 Nutation

Consider a force-free symmetric gyroscope with no torques acting on it. As expected, the angular momentum is conserved and its direction points to a fixed direction in the laboratory system. As the angular velocity is parallel to the rotation axis, both angular velocity and angular momentum are parallel to the figure axis. The gyro disk rotates around a fixed axis. As the gyroscope's behavior is examined in the situation of a temporary impulse, angular velocity and angular momentum are not parallel. In this case, Euler's Equations (Eq. 9 - Eq. 11) state:

$$\begin{aligned} I_1\frac{d\omega_1}{dt} + (I_3 - I_1)\omega_2\omega_3 &= 0 \\ I_2\frac{d\omega_2}{dt} + (I_1 - I_3)\omega_3\omega_1 &= 0 \\ I_3\frac{d\omega_3}{dt} &= 0 \end{aligned}$$

With the relation:

$$\omega_P = \frac{I_1 - I_3}{I_3}\omega_1, \tag{25}$$

It implies that:

$$\frac{d\omega_1}{dt} + \Omega_P\omega_2 = 0 \tag{26}$$

$$\frac{d\omega_2}{dt} - \Omega_P\omega_1 = 0 \tag{27}$$

$$\frac{d\omega_3}{dt} = const \tag{28}$$

Such that:

$$\vec{\omega} = \begin{bmatrix} \omega_\perp cos(\omega_P t) \\ \omega_\perp sin(\omega_P t) \\ \omega_3 \end{bmatrix} \text{ and } \vec{L_P} = \begin{bmatrix} I_1\omega_\perp cos(\omega_P t) \\ I_1\omega_\perp sin(\omega_P t) \\ I_3\omega_3 \end{bmatrix} \tag{29}$$

Where:

$$\omega_P = \text{Precession Frequency}(s^{-1})$$

This implies that the angular velocity axis (the rotation axis) precesses on a cone around the figure axis. This cone is called the ***polhode cone***. The absolute value of the angular velocity is given by:

$$\omega = \sqrt{\omega_\perp^2 + \omega_3^2}$$

On the other hand, the projection of the angular velocity onto the direction of the angular momentum is given by [3]:

$$\omega_1^2 + \omega_2^2 + \omega_3^2 = \frac{L}{I_1} + \frac{L}{I_3} = const \tag{30}$$

The angle between the rotation axis and the direction of the angular momentum remains constant. As the angular velocity changes over time, it precesses on a cone around the angular momentum direction. This cone is known as the ***herpolhode cone*** [3]. Consequently, the figure axis moves around the angular momentum direction, and the polhode cone rolls on the herpolhode cone. The combined motion of the figure axis and the instantaneous rotation axis is referred to as ***nutation*** [2]. The half-opening angles of the polhode cone and the nutation cone can be derived from the angles formed between the angular velocity or angular momentum and the figure axis. The half-opening angle of the nutation cone is given by:

$$\alpha = \tan^{-1}(\frac{I_1\omega_\perp}{I_3\omega_3}) = \tan^{-1}(\frac{L_{P\perp}}{L_{P\parallel}}) \tag{31}$$

and the half-opening angle of the polhode cone by:

$$\beta = \tan^{-1}(\frac{\omega_\perp}{\omega_\parallel}) = \tan^{-1}(\frac{\omega_\perp}{\omega_3}) \tag{32}$$

In the case of a prolate gyroscope where $I_1 > I_3$, the opening angle of the nutation cone is larger than that of the polhode cone. As Fig. 2.5 shows, the three different motions are strongly correlated:

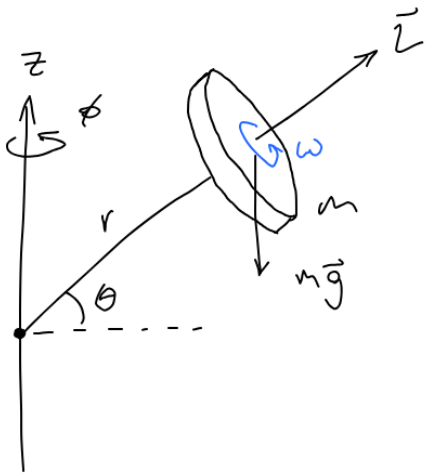

Figure 1: Motion of a disk gyroscope.

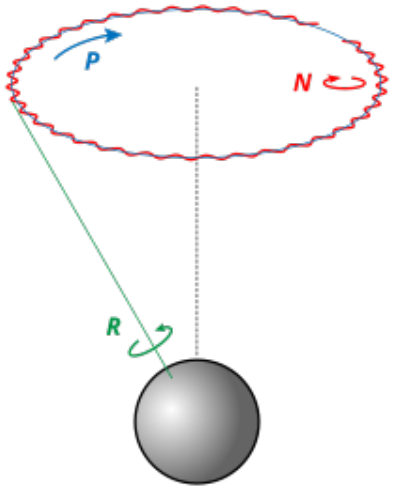

Figure 2: Motion of a sphere gyroscope.

3 Task I - Determining I_3

3.1 Experiment Setup

For the first experiment, the system was setup with the gyroscope positioned horizontally, fixed by the additional stand rod to prevent rotation about the z-axis. The string is wrapped around the bobbin and a weight is attached to the other end of the spring.
I_3 was determined via three different methods, through; angular acceleration α with use of Eq. 15, through the rotational speed ω with use of Eq. 16 and also a theoretical I_3 calculated from the Eq. 4.

The initial conditions:

$$\text{Mass of the Weight} = m_W = 47 \times 10^{-3} kg$$
$$\text{Radius of the Disk} = R = 125 \times 10^{-3} m$$
$$\text{Radius of the Bobbin} = R = 32.5 \times 10^{-3} m$$
$$\text{Initial Height} = h = 1m$$

3.2 Data Analysis

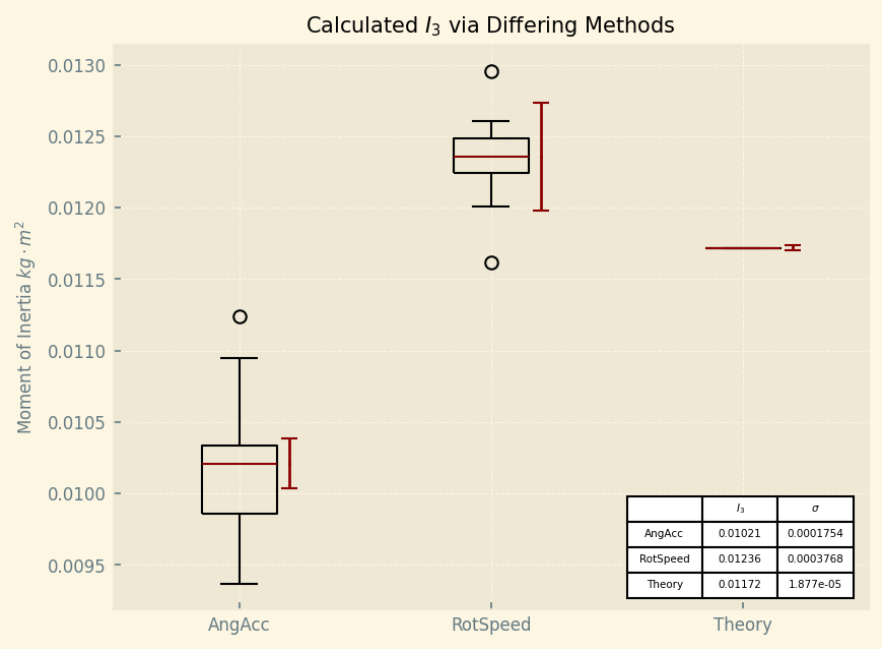

Figure 3: Moment of Inertia of a Disk.

Figure 3 compares the values of moment of inertia of the gyroscope, using the three different computational methods through use of α, ω and theoretical literature [3], Equations Eq. 15, Eq. 16 and Eq. 4 respectively. The moment of inertia determined by the α is $I_3^{\alpha} = (0.01021 \pm 1.754 \cdot 10^{-4}) Kgm^2$ or an percent error of 1.715%. Through the ω calculation $I_3^{\omega} = (0.01236 \pm 3.768 \cdot 10^{-4}) Kgm^2$ which had the highest uncertainty and a percent error of 3.05%. Comparing the two I_3 derived from the measured data they both fail the encompass the theoretical value $I_3^T = (0.01172 \pm 1.877 \cdot 10^{-5}) Kgm^2$, however, I_3^{ω} and I_3^{α} both have fringe data points outside their minimal lower quartile(Q_1) and maximal upper quartile(Q_3) values respectively that are comparatively similar to I_3^T. It is also of note that I_3^T has a percent error of 0.16% that arises from uncertainty in measurement values.

4 Task II - Damping constant and friction coefficient

4.1 Experiment Setup

Measure the deceleration of the gyro by friction. Determine the friction coefficient. The next condition that was explored was an extended duration of rotation, wherein the gyroscope was setup as in section 3.1 and a pull cord was wound around the bobbin and subsequently pulled, generating a large ω_0. The rotational speed was then periodically measured, every 10s over the course of 120s as the gyroscope slowed down. Providing a times series of rotational speeds $\omega(t)$ that reflected a gradual deceleration due to frictional forces acting on the gyroscope. Eq. 18 was then used to determine the damping constant b and further analysis was conducted to determine $\mu(\omega)$.

4.2 Data Analysis

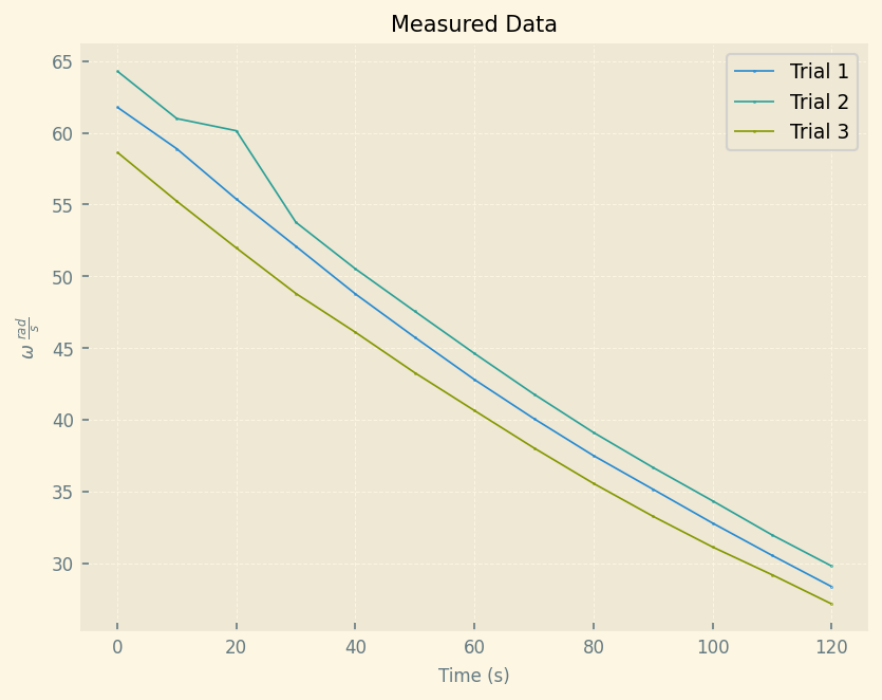

Figure 4: Measured data across three trials

Fig. 4 shows the measured ω over a duration of 120s. Each Trial shows a similar downwards decaying envelope that appears exponential in nature. Trial 2 has a data point that significantly deviates from the overall trend of its data and although initially it can be perceived as an outlier, the value is not unnatural, *(i.e. greater than its previous or lower than its subsequent values)* nor was there a determined experiment mishap or fault when recording that particular data point. Thus the data point was considered in further analysis.

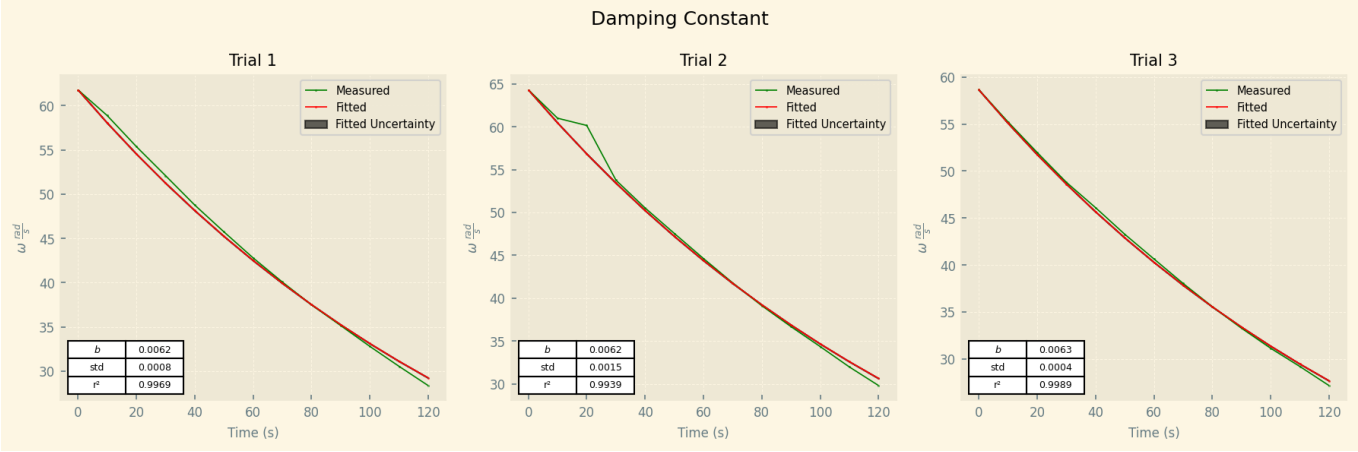

Figure 5: Damping constant of each Trial

Through use of Eq. 18 or each trial a damping constant b was determined Fig. 5 through a curve-fitting analysis. Each trial its respective r^2-value is significantly high and the margin of error significantly low with an error percent for Trials 1,2,3 of 12.90%,24.19%,6.35% respectively. The damping constant of each trial was then averaged for a final damping constant $b = (0.006223 \pm 4.5 \cdot 10^{-5})s^{-}1$ with an error percent 12.90%.

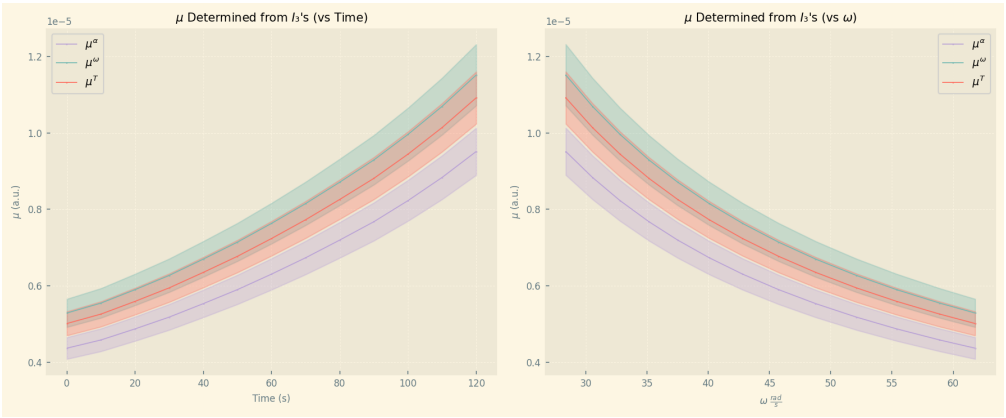

Figure 6: Measured data across three trials

Upon initial view of Fig. 6 the friction coefficient across all μ^X is a small value on the order of 10^{-5}. Also seen is the frictional coefficient $\mu(\omega)$ for each moment of inertia $I_3^{\alpha}, I_3^{\omega}, I_3^{T}$ calculate in section 3.2. Across all calculated friction coefficients against time exponentially increase as the time increases, which when comparing to μ and ω shows that overtime the initial low frictional coefficient of $\mu^X \approx (0.42 - 0.55)10^{-5}$ and high ω causes a slight decrease in ω which increases μ and so forth creating a exponentially increasing μ^X overtime across all inertia's used. Inversely Fig. 6 also shows that as $\log(\omega)$ increases the $\log(\mu)$ decreases.
When comparing μ^{ω} and μ^T each are closer to the other than each is to $\mu\alpha$. Both also fall within the error bands of each other suggesting this the method used in μ^{ω} may posses a level accuracy about the μ^T for this gyroscope however, further analysis is required.

5 Task III

Measure the precession frequency as a function of the rotation frequency of the gyro disk for two different torque values. Plot the precession frequency in an appropriate manner as a function of the rotation frequency and determine the value of the moment of inertia component I_3.

5.1 Experiment Setup

For the next experiment, the fixation of the gyroscope to the stand is removed, allowing the gyroscope's axis to be free. Using counterweights, the gyroscope axis is carefully balanced until it achieves indifferent equilibrium. This ensures that the axis remains balanced at any inclination relative to the horizontal, minimizing unwanted torque effects that could disturb the experiment. Then the gyroscope is brought to an initial stable point with no precession with use of the pull cord. Using a stopwatch and two weights of masses $m_1 = 47g$ and $m_2 = 94g$, a weight is place on the gyroscope at a distance z_z from its axis of precess the time for half of a precession period is recorded, this is repeated for m_2. This is done by timing the duration it takes for the gyroscope to move through a 180° arc of its precessional path. initial conditions are needed for calculations are:

$$\text{Mass of the Disk} = M = 1.5kg$$
$$\text{Mass of the Counterweights} = m_b = 1.4kg \text{ and } m_s = 50 \times 10^{-3}kg$$
$$\text{Radius of applied torque by Weight} = z_z = 190 \times 10^{-3}m$$

A torque was torque based on initial conditions for each mass and the precession frequency was plotted against the inverse of the rotation frequency. Through use of Eq. 22 and linear regression, the parameter p determined from the linear regression is:

$$\Omega_p = \frac{M}{L} = \frac{m_z g z_z}{I_3 \omega} = \frac{p}{\omega} \tag{33}$$

$$p = \frac{m_z g z_z}{I_3} \implies I_3 = \frac{m_z g z_z}{p} \tag{34}$$

Thus I_3 was subsequently determined.

5.2 Data Analysis

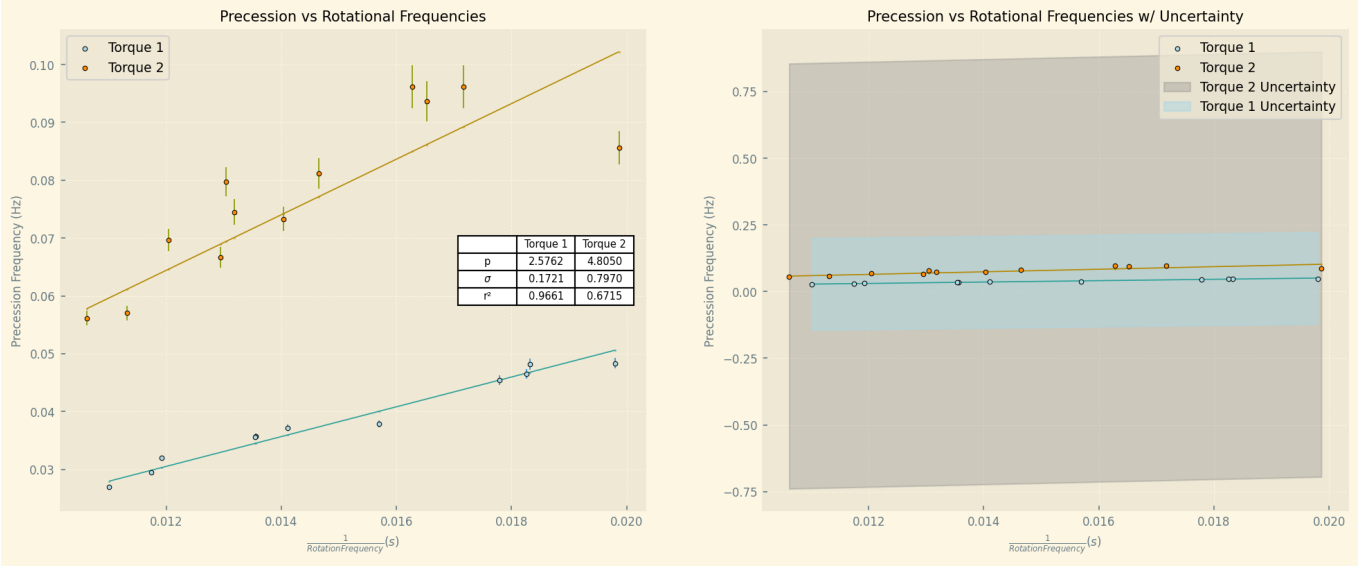

Figure 7: Precession Frequency vs Rotational Frequency

It is apparent when viewing Fig. 7 that the uncertainty of the fitted results was significantly large, this is a result of the difficulty in capturing measurements, which primarily relied on too not only stop a timer and record the rotational speed after half period but also to consistently determine by eyesight where that half period was. It is also of note that because only a half period was measured this result in an uncertainty that is twice is high than if a full period was measured. The lesser torque, Torque 1 resulted in a $p_1 = (2.5762 \pm 0.1721)s^{-2}$ with $r^2 = 0.9961$ that strongly agrees with measured data. Torque 2 in comparison was found to have $p_2 = (4.8050 \pm 0.7970)s^{-2}$ that shows weak correlation with measured data with $r^2 = 0.6715$.

	$I_3(Kgm^2)$	$\sigma(Kgm^2)$
Torque 1	0.03043	$\pm$0.002033
Torque 2	0.03263	$\pm$0.005411

Table 1: Determined I_3 from Precession Frequency

From Table 1 the determined I_3 for Torque 1 and Torque 2 were found to be $I_3^1 = (0.03043 \pm 0.002033)Kgm^2$ and $I_3^2 = (0.03263 \pm 0.005411)Kgm^2$ respectively it is notable the through the calculation of I_3^X the large uncertainty from p_X did not significantly impacted the uncertainty of the final inertia's. It is also of note the uncertainty of each Inertia calculated encompasses the Inertia value of the other, suggesting that they are in agreement.

6 Task IV

6.1 Experiment Setup

For the last experiment, the gyroscope is mounted so it can rotate freely. To stabilize the setup, counterweights are adjusted until the gyroscope's axis is in equilibrium, as before. After setting the gyroscope to a target rotation speed, a brief vertical impulse is applied to the gyroscope axis to initiate nutation. This impulse produces a small angular displacement α, where the gyroscope's axis oscillates vertically, due to its moment of inertia. the duration for the α to oscillate three times was measured along with the average rotational speed, ω during this time. Through use of Eq. 25 and Eq. 31, the inertia introduced by the vertical impulse I_1 was determined.

6.2 Data Analysis

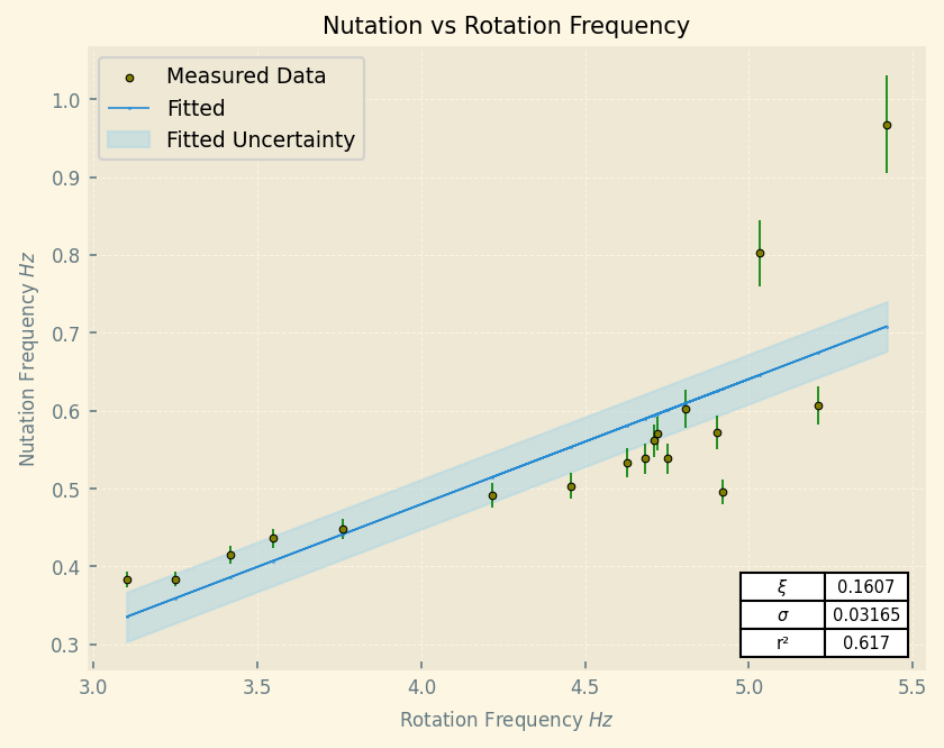

Figure 8: Nutation vs Rotation Frequency

The results of Fig. 8 weakly suggest that there is linear relationship between the rotation frequency and the nutation frequency. With the data collected there was two data points that deviated significantly from the trend of the remaining data points however as previously mentioned there was no logical reason the discard these points thus they remained in the data set. However it is predicted that the large variation of these two points from the rest of the data set is a result of the errors encountered when measuring the data. particularly in measuring the angle α by eyesight over the course of three oscillations. However these result may also be attributable to additional chaotic behavior occasionally encountered at high oscillation angles α. Further analysis is required. An ξ of 0.1607 ± 0.03165 however this result is weakly correlated with measured data, $r^2 = 0.617$.

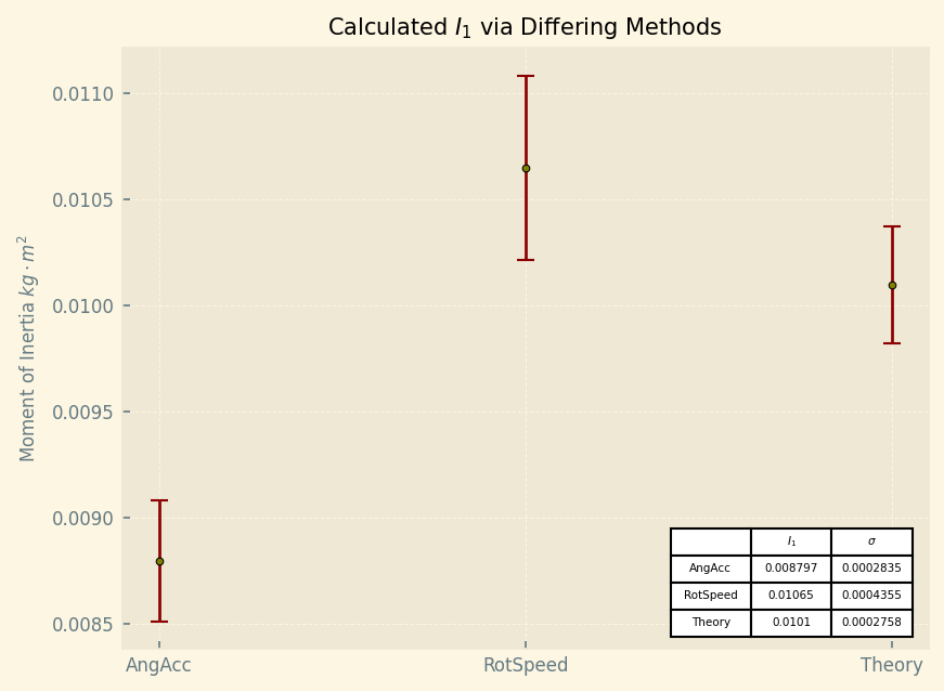

Figure 9: Calculated I_1 across I_3^{α},I_3^{ω},I_3^{T}

Plotting the calculated I_1 across each I_3 determined in section 3.2 it is apparent there is a large range that encompasses all results $\approx (0.0087 - 0.0106) Kg \cdot m^2$. Further, the error in $I_1^{\omega} = (0.01065 \pm 4.355 \cdot 10^{-4}) Kgm^2$ and $I_1^{T} = (0.0101 \pm 2.758 \cdot 10^{-4}) Kgm^2$ just overlap on the respective fringes of each, suggesting little correlation across methods used. $I_1^{\alpha} = (0.008797 \pm 2.835 \cdot 10^{-4}) Kgm^2$ is significantly distant from the other two values and has no correlation across the other methods. The large error across all determined inertia's in Fig. 9 show little precision in the values determined.

7 Discussion and Conclusion

This study investigated the rotational dynamics of a gyroscope. The goal of this report was to understand the physics of gyroscopic motion through differing scenarios and further compare measured data with theoretical values and common standing literature. Overall the report was able to make comparison to literature values across each experiment, and the trend was that the results of the data did not suggest a strong correlation with theoretical measures.
the results of experiment 1 in Figure 3 present a comparative analysis of the gyroscope's moment of inertia values derived from three different computational methods. Specifically, these methods are based on angular acceleration (α), angular velocity (ω) and a theoretical value [3], applied through Eqs. 15, 16 and 4 respectively. The moment of inertia value derived via angular acceleration I_3^{α} was calculated as $(0.01021 \pm 1.754 \cdot 10^{-4}) Kgm^2$ with a relatively low percent error of 1.715%. This method suggests values with a high degree of precision, although the computed values remain slightly below the theoretical values. The angular velocity method I_3^{ω} has a higher moment of inertia, with values as $(0.01236 \pm 3.768 \cdot 10^{-4}) Kgm^2$ though it carries a larger uncertainty and a percent error of 3.05%.

Despite this both experimental values approaching the theoretical value $I_3^{T} = (0.01172 \pm 1.877 \cdot 10^{-5}) Kgm^2$ neither reaches I_3^{T} within their respective error ranges, indicating a systematic discrepancy or potential error within the procedure. However, some fringe data points of I_3^{ω} align closely with I_3^{T}, implying that perfected measurements or modified approaches may improve accuracy.

In Figure 4, the behavior of ω is captured over a 120-second interval, expressing a consistent downward decay across all trials. Trial 2 contains a data point that deviates significantly from the expected exponential decay trend. Initially, this point seemed having an unique behavior, but it was considered

for further analysis, as no experimental mistake was observed during its recording.

Through the application of Eq. 18, a damping constant b was determined for each trial by fitting the exponential decay curve into the data. High values across trials indicate correlations and the errors remain minimal, though the percent error for the damping constant varies, with Trial 1 at 12.90%, Trial 2 at 24.19% and Trial 3 at 6.35%.The averaged damping constant across trials was calculated as $b = (0.006223 \pm 4.5 \cdot 10^{-5})s^{-}1$, with an error percent of 12.90%, providing an estimate for frictional dissipation in the gyroscope system that its self models the data collected, further analysis with b was performed to determine the frictional coefficient ($\mu(\omega)$).

In Figure 6, the progression of the friction coefficient μ^x consistently remains on the order of 10^{-5}, underscoring the gyroscope's high rotational stability. The friction coefficient calculated for each inertia value demonstrates a steady increase over time, attributed to the interplay between diminishing angular velocity and the corresponding rise in frictional effects. This is a expected result when considering the model used, however what is of note is the comparably low error bands *(significantly high precision)* present in Fig. 6 across all frictional coefficients calculated. In conjunction with μ^ω and μ^T crossing the error band of each other suggests a level of accuracy about a central value.

Experiment 3 produced Figure 7 which reflects significant uncertainty in the fitted results, attributed to the difficulty in capturing precise measurements through manual processes of timing and identification of the half-period by eye. Furthermore, as only a half-period was measured, the uncertainty was amplified compared to a full-period measurement. The decay parameter for Torque 1 was calculated as $p_1 = (2.5762 \pm 0.1721)\,\mathrm{s}^{-2}$ with $r^2 = 0.9961$, indicating a strong correlation. In contrast, Torque 2 produced $p_2 = (4.8050 \pm 0.7970)\,\mathrm{s}^{-2}$ which shows a weaker correlation at $r^2 = 0.6715$. Both of these correlations, suggest an inverse relationship between the rotational frequency of the gyroscope and its precession about the z-axis.

The final experiment explored the disturbance, or nutation of the gyroscope as a result of a vertical impulse. Figure 8 shows a weak linear relationship ($\xi = (0.1607 \pm 0.03165)$ with $r^2 = 0.617$, observed between the rotation frequency and nutation frequency. Two significant outliers were retained in the data set, as there was no apparent rationale for discarding them. The deviations may stem from measurement error, particularly in manually assessing the angle α over three oscillations, although chaotic behavior at high α values could also be a factor.

The determined ξ was utilized to calculate I_1 values across all I_3 calculated in section 3.2. The results, Fig. 9 when considering all I_1's calculated spanned a broad range $\approx (0.0087 - 0.0106)Kg \cdot m^2$, with Minimal overlap existing between errors, only for $I_1^\omega = (0.01065 \pm 4.355 \cdot 10^{-4})Kgm^2$ and $I_1^T = (0.0101 \pm 2.758 \cdot 10^{-4})Kgm^2$, while $I_1^\alpha = (0.008797 \pm 2.835 \cdot 10^{-4})Kgm^2$ showed no correlation with other methods. This differences in inertia values, along with large error margins, underscores a lack of precision in the measurements and suggests the need for improved measurement techniques or additional trials for more reliable data.

References

[1] Y. D. Hugh and R. A. Freedman. Dynamics of rotational motion. In *University with Modern Physics*, pages 330–355. Pearson, 15th edition, 2020.

[2] Wikipedia. Precession. https://en.wikipedia.org/wiki/Precession, 2024. Accessed: 2024-11-12.

[3] M. Ziese. *M06e Gyroscope with three Axes.* Universität Leipzig, October 2024.